CARBON 46 (2008) 537–543

available at www.sciencedirect.com

ScienceDirect

journal homepage: www.elsevier.com/locate/carbon

# First principle calculations of the electronic properties of nitrogen-doped carbon nanoribbons with zigzag edges

*S.S. Yu, W.T. Zheng*, Q.B. Wen, Q. Jiang*

*Department of Materials Science, State Key Laboratory of Superhard Materials, and Key Laboratory of Automobile Materials, MOE, Jilin University, Qianjing Road 2699, Changchun 130012, PR China*

ARTICLE INFO

*Article history:*
Received 25 September 2007
Accepted 7 January 2008
Available online 16 July 2008

ABSTRACT

Calculations have been performed for carbon nanoribbons (CNRs) with zigzag edges containing one substitutional nitrogen atom per 154 carbon atoms, using ab initio density functional theory. It is found that the formation energies of these nanoribbons depend on the nitrogen doping site, as do the electrical properties. The doping nitrogen atom energetically prefers to distribute near the nanoribbon edges, and there is an impurity state below or above the Fermi level for the nitrogen-doped CNR, which depends on the nitrogen doping site. Also, the distribution of non-bonding electrons of nitrogen atom depends on the nitrogen doping site.



## 1. Introduction

Nanometric carbon materials exhibit various remarkable properties depending on their geometry. Among them, CNRs are nanometer-sized stripes of graphene sheets, in which the boundary regions play an important role [1]. Due to their structural resemblance to carbon nanotubes and having the quantum confinement effects, CNRs are expected to present electronic properties similar to those of carbon nanotubes which can be unwrapped into CNRs [2,3]. However, some theoretical studies show that the metallic or semiconducting feature in CNRs is different from that in carbon nanotubes [1,4,5]. The electronic properties of nanoribbons are ruled by the width and atomic geometry along the edge, namely, zigzag or armchair. Similar to armchair nanotubes, CNRs with zigzag edges are all metallic, while for CNRs with armchair edges, the band-gap oscillations have been presented as a function of their width [6–8]. That is to say, CNRs can be made either as metallic or as semiconducting materials by controlling their width or angle between the hexagons and the ribbon axis [9]. For CNR with zigzag edges, the existence of a very large density of states at the Fermi level, which is attributed to the edge localized states having non-bonding character [1], was predicted with tight-binding model [3,8,9] and first-principles calculations [5,10,11]. The unpaired $\pi/\pi^*$ edge electrons give rise to a magnetic ordering on the system [6,12]. Hence, the Pauli ferromagnetic susceptibility should be an important component in CNR with zigzag edges [1,13]. However, CNR with armchair edges is diamagnetic susceptibility since it has a zero density of states at the Fermi level.

Several experimental groups have successfully produced isolated and stable 2D crystals of graphene at room temperature [14–16]. Scanning tunneling microscopy (STM) images of graphene sheets have revealed bright stripes along its edges, suggesting a high density of edge states near the Fermi level [17,18]. Graphene is a semimetal at the micron scale or larger, but when it is trimmed down to less than 100 nm, electron confinement opens its band-gap, resulting in an effect that can be used to tune the crystal's electronics for different purposes [19]. CNR has attracted enormous attention due to fundamental scientific interest in nanomaterials and its versatile electronic properties that are expected to be important for future application in nanoelectronics [6]. In addition, due

* *Corresponding author:* Fax: +86 431 85168246.
E-mail address: wtzheng@jlu.edu.cn (W.T. Zheng).
0008-6223/$ - see front matter 
doi:10.1016/j.carbon.2008.01.006

to the flat structure, CNRs are much easier to manipulate than carbon nanotubes [2,20].

It is well known that the mechanical and electronic properties of carbon materials can be controlled through the incorporation of impurities [21]. N atom or B atom is the idea substitutional impurities as it has roughly the same atomic radius as C, while it possesses one electron more or less than C. The graphite-like $CN_x$ such as pyridine-like nitrogen, triplebonded CN and substitutional nitrogen in graphite as well as BN with only $sp^2$ bonding has been reported [22–26]. In particular, N-doped fullerenes have been found to exhibit a high hardness combined with a high elasticity due to cross-linking between curved basal planes [27]. Likewise, N doping of carbon nanotube [28] can give rise to nanotube functionalization [29] and other changes in the structure [30,31]. When one nitrogen atom or one boron atom is incorporated into carbon nanotube, there will be an impurity level near the bottom of the conduction band or the top of the valence band. Consequently, the nanotube is transformed from intrinsic semiconductor to *n*-type or *p*-type semiconductor [32–37]. Also, when CNRs are doped with boron atoms, the boron impurities can also affect the nanoribbon metallic behavior and break the polarized transport degeneracy [13]. And, the conductance of CNR doped with a non-magnetic impurity strongly depends on the position and strength of the impurity [38]. However, up to now, there are no reports about how the doping site influences the electronic properties of CNRs with zigzag edges doped with magnetic impurity. In this work, we have investigated electronic properties of CNRs doped with nitrogen atom at different sites with hydrogen passivated zigzag edges in detail.

## 2. Methods

We used the code DMOL3 based on the density-functional theory (DFT) available from Accelrys Inc. [39,40]. In this code, each electronic wave function was expanded in a localized atom-centered basis with each basis defined numerically on a dense radial grid. All-electron calculations were performed with a double numeric plus polarization basis (DNP) set. For the exchange and correlation term, the generalized gradient approximation (GGA) was used as proposed by Perdew–Burke–Ernzerhof (PBE) [41] and a finite basis cutoff of 3.7 Å was adopted. C–C bond length of 1.42 Å was chosen before geometry optimization. The formation energy $E_f$ of N-doped CNRs is calculated using the following equation:

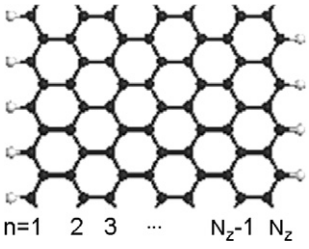


**Fig. 1 – Schematic of ZCNR. The grey balls denote hydrogen atoms passivating the edge carbon atoms and the black balls represent carbon atoms in the nanoribbon structure.**

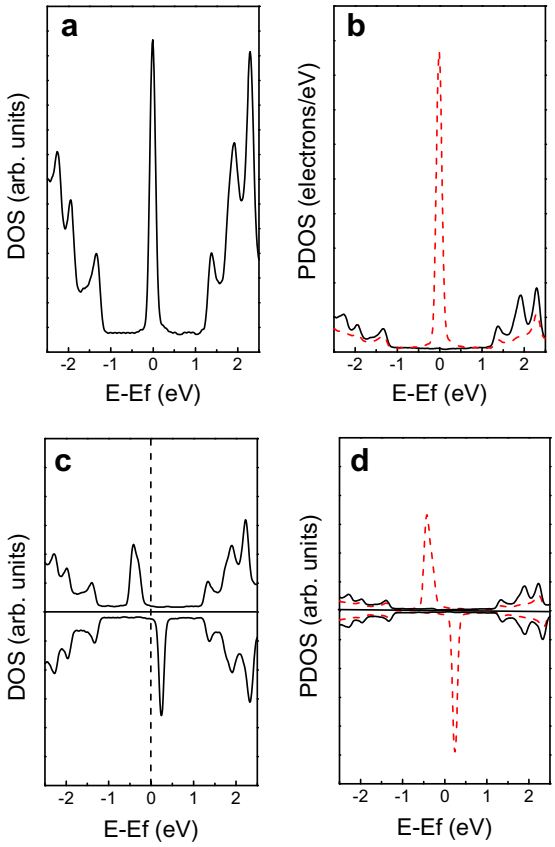


**Fig. 2 – The electronic structures for the 7-ZCNR are plotted: (a) and (c) the total density states and (b) and (d) partial density states for one carbon atom in the inner (solid line) and edge of ribbon (dashed line). (a) and (b) are treated with spin-restricted DFT, while (c) and (d) are calculated with spin-polarized DFT.**

$$E_f = (Et_1 + E_2) - (Et_2 + E_1), \quad (1)$$

where $Et_2$ is the total energy of perfect CNR, $Et_1$ is the total energy of CNR with substitutional nitrogen atoms, $E_1$ and $E_2$ are the energies of single free nitrogen and carbon atom, respectively.

To mimic a situation of an isolated CNR, we adopted three-dimensional repeating supercells in which individual ribbons are separated by a vacuum region. In the adopted vacuum

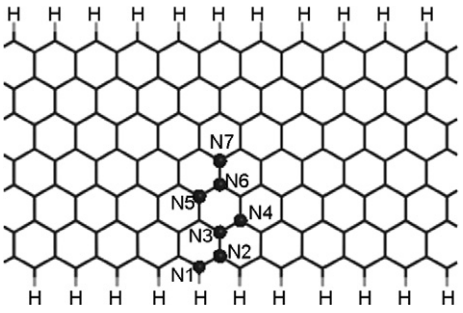


**Fig. 3 – Schematic of different substitutional sites in a structural model of hydrogenated 7-ZCNR doped with one nitrogen atom per 154 carbon atoms.**

**Table 1 – The total energy differences for the hydrogenated 7-ZCNR with one substitutional nitrogen atom per 154 carbon atoms**

| Configuration | N2 | N3 | N4 | N5 | N6 | N7 |
|---|---|---|---|---|---|---|
| ΔE (eV) | 1.14 | 1.00 | 1.39 | 1.30 | 1.44 | 1.41 |

$\Delta E = E_i - E_{N1}$, i = N2–N7.

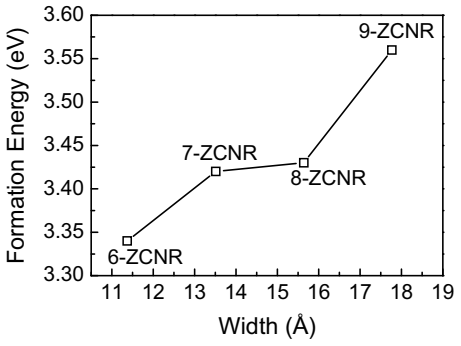


**Fig. 4 – Formation energies of N-doped $N_z$ -ZCNR depend on the ribbon width, when one substitutional nitrogen atom in the supercell (27.07 Å) locates at the ribbon edge.**

region, the intervals among the ribbons were kept as 10 Å for both edge-edge and layer-layer distance. These intervals were enough to ensure negligible interaction between the ribbon and its periodic images. The length of CNR with zigzag edges was chosen as 27.07 Å. The positions of all the atoms including the doping nitrogen atoms and passivated hydrogen atoms in the supercell were not constrained and could be fully relaxed under the condition that the cell parameters were fixed on the values optimized for the original supercell.

Following previous convention [1,3–8], the CNRs with zigzag edges on both sides are classified by the number of the zigzag chains ($N_z$) across the ribbon width, as shown in Fig. 1. We refer to a CNR with $N_z$ zigzag chains as a $N_z$-ZCNR. In this work, we present a theoretical description of electronic properties of 7-ZCNR containing 154 carbon atoms and 22 passivated hydrogen atoms.

## 3. Results and discussion

First, we treated the hydrogenated 7-ZCNR as a closed-shell system with spin-restricted DFT, whose electronic structures are plotted in Fig. 2a and b. From the density of states (DOS) in Fig. 2a, we can see that the 7-ZCNR is metallic, which is similar to armchair carbon nanotube. However, for the 7-ZCNR, there is a remarkably sharp peak which is bisected by the Fermi level. In Fig. 2b, the solid and dash lines are partial density states (PDOS) for one carbon atom in the inner of ribbon and at the edge of ribbon. It is clear that the sharp peak comes from the edge state contributed by the unpaired π edge electrons, which results from a quantum confinement effect depending on the ribbon width [3]. The results are the same as those predicted with tight-binding model [3,8,9] and first-principle calculations [5,10,11]. Due to the existence of the magnetic moment at the edge [1,6,12,13] for the hydrogenated 7-ZCNR, the spin-polarized DFT is employed, whose

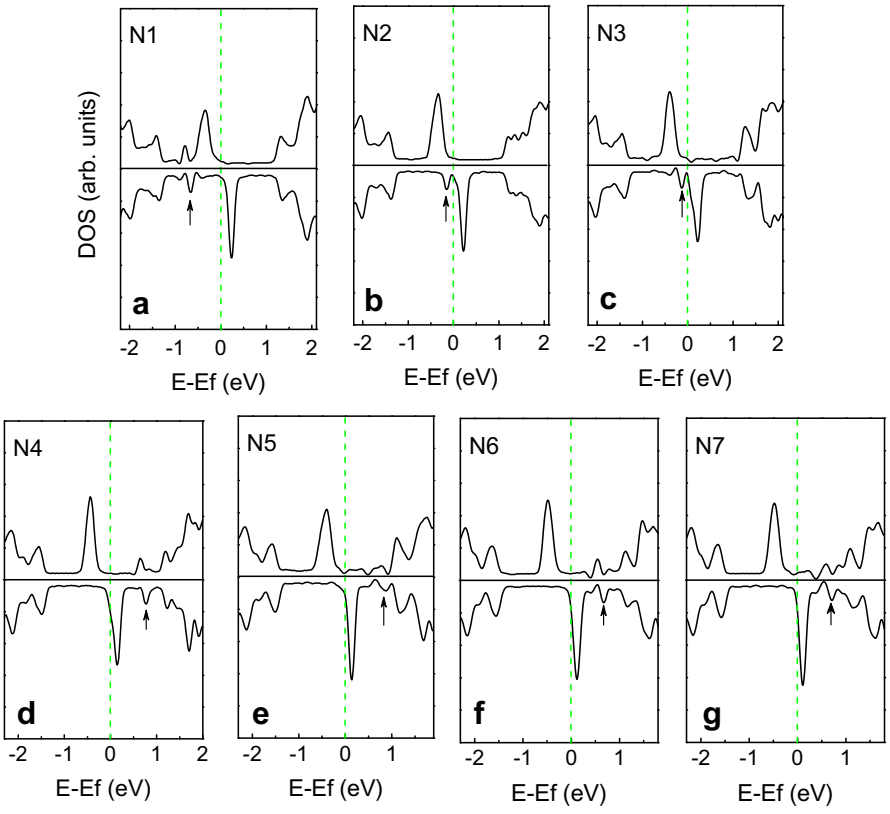


**Fig. 5 – The electronic density of states (DOS) for N1–N7 configuration.**

electronic structures are plotted in Fig. 2c and d. A remarkably sharp peak at the Fermi level in Fig. 2a splits up into two striking peaks, as shown in Fig. 2c. As a result, the two spin states shift in the opposite direction relative to the Fermi level, which is also consistent with previous calculations [13,42]. The splitting between spin-up and spin-down π-orbital states at the Fermi level demonstrates that ZCNRs are ferromagnetic [6,13]. In Fig. 2d, the solid and dash lines are PDOS for one carbon atom in the inner of ribbon and at the edge of ribbon, which shows that the ferromagnetic state comes from the edge state. It is energetically favorable compared with the non-magnetic configuration (about 5 meV/edge-atom lower) since there is an enhance exchange splitting of the localized π-orbital states at the Fermi level [13], as shown in Fig. 2c.

Nitrogen atoms can be incorporated into the hexagonal network of ZCNRs through the substituting carbon atoms. 7-ZCNRs containing one substitutional nitrogen atom in the supercell containing 154 carbon atoms are considered. It means that one substitutional nitrogen atom corresponds to one nitrogen concentration of 0.6%. From the edge to inner, we investigate seven configurations for the hydrogenated 7-ZCNR with a substitutional nitrogen atom, denoted by N1–N7, as indicated in Fig. 3. Their corresponding total energies ($E$) are compared as listed in Table 1. It can be found that configuration N1 is the most energetically favorable, which means that nitrogen prefers to be at the edge of nanoribbons for the hydrogenated ZCNR. N2 and N3 are comparatively preferable, while N6 and N7 are the most unfavorable. The special edge state strongly depends on the ribbon width [3]. The edge state is very important when the ribbon width is of nanoscale size. Fig. 4 demonstrates the formation energy depending on the ribbon width, when the substitutional nitrogen atom locates at the ribbon edge. With increasing ribbon width, the formation energy also increases.

The electronic density of states for the hydrogenated 7-ZCNR containing one nitrogen atom per 154 carbon atoms

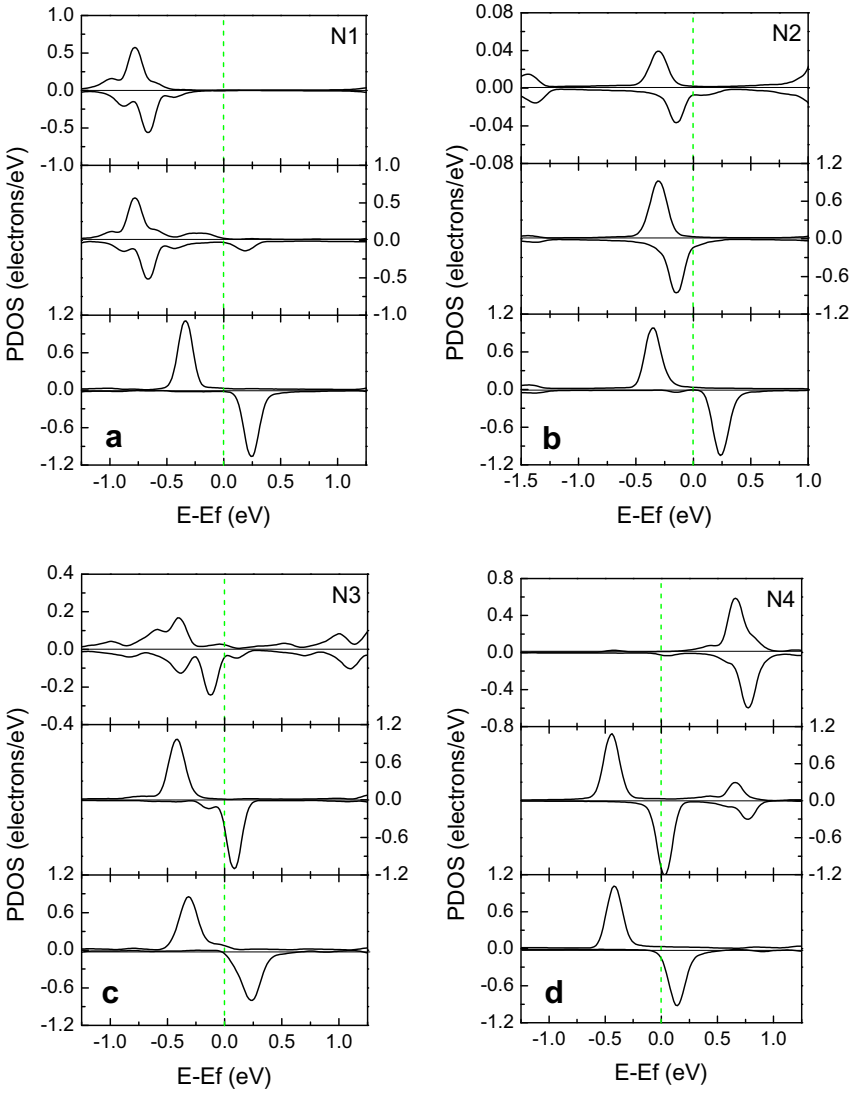


**Fig. 6 – The electronic partial density of states (PDOS) for N1–N7 configuration. The top panel is PDOS of the nitrogen atom, the middle one PDOS of the edge C atom whose distance from the nitrogen atom is the shortest, and the bottom one PDOS of the edge C atom whose distance from the nitrogen atom is the longest.**

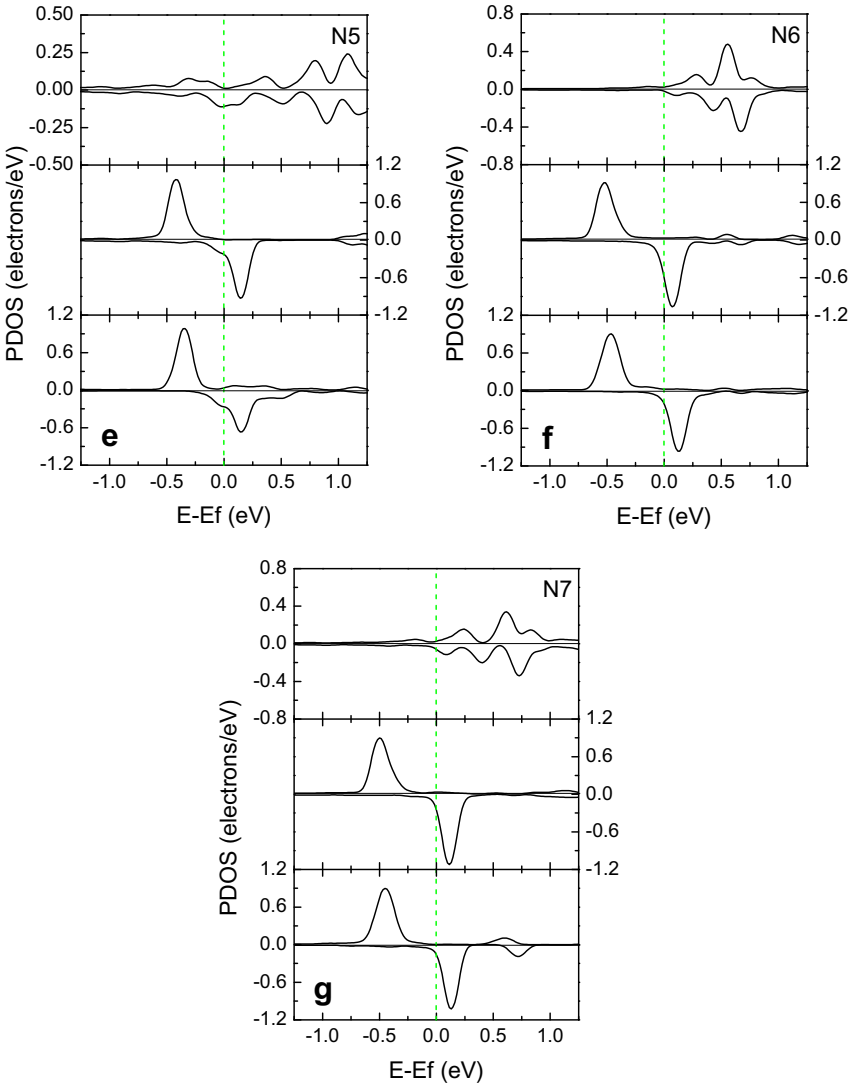


**Fig. 6 – (*continued*)**

at different sites are shown in Fig. 5, which are similar to that of perfect 7-ZCNR (Fig. 2c). It is worth noting that remarkably splitting sharp peaks all appear near the Fermi level. However, it is observed that there is one striking splitting impurity state, marked by arrow, for each one nitrogen-doped 7-ZCNR, as shown in Fig. 5. For N1, N2 and N3 configuration, the impurity state lies below the Fermi level, while for N4, N5, N6 and N7 configuration, the impurity state locates above the Fermi level. This indicates that nitrogen and its location affect the electronic properties of the ZCNR significantly. For N2 and N3 configuration, the spin-up impurity states and the spin-up edge states near the Fermi level are almost degenerate. It is noted that the splitting width of spin-up and spin-down impurity states is smaller than that of the edge states at the Fermi level. On the other hand, the impurity state of N1 shows a farther away below the Fermi level than other configurations, as shown in Fig. 5. This is why the total energy of N1 is lower than that of other configurations.

It is well known that nitrogen atom has one extra electron in comparison with carbon atom. For nitrogen-doped carbon nanotubes, the extra electron mainly lies around the nitrogen atom and give rise to a donor state near the Fermi level [29,37]. For 7-ZCNRs doped with one nitrogen atom per 154 carbon atoms at different sites, their PDOS are exhibited in Fig. 6. The top panel is the PDOS for nitrogen atom, the middle one the PDOS for carbon atom at the edge whose distance from nitrogen atom is the shortest among the carbon atoms at the edge, and the bottom one also the PDOS for carbon atom at the edge whose distance from the nitrogen atom is the longest. It is clear that the extra electron of nitrogen atom occupies the spin-down states. The energy level of impurity states depend on both the coulomb attraction of $N^+$ and the correlation of unpaired $\pi$ edge electrons with the extra non-bonding electron in N atom, and the distance between the nitrogen atom and the ribbon edge decides to the sign change of the impurity energy level. (The energy level of impurities for N3 is at threshold of this sign change.) When the nitrogen atom lies at the edge, due to the strong interaction between the extra non-bonding electron and $N^+$, the impurity state locates below the Fermi level (the energy level of impurity states are negative). However, when the nitrogen atom locates far away the edge, the correlation of unpaired spin-up $\pi$ edge

electrons with the extra non-bonding electron is stronger than the coulomb attraction of $N^+$, leading to that this extra non-bonding electron tends to appear at the edge atoms and occupy the lowest unpaired $\pi^*$ edge electron level, which uplifts the Fermi level. Since $N^+$ has a strong ability to attract $\pi$ electrons of its neighboring C atom, the center of negative charge around the $N^+$ has been formed, which can introduce the impurity state above the Fermi level (the energy level of impurity states are positive).

For N1 configuration, due to the extra non-bonding electron tightly around $N^+$, the impurity spin-down state coupling with edge spin-up state locates far away the Fermi level. With increasing the distance between nitrogen atom and edge, the extra non-bonding electron is weakly restricted around $N^+$. Hence, the impurity state of N2 is more near the Fermi level than N1. However, for transition configuration N3, there two states that can be occupied by the extra non-bonding electron. One is the impurity state below the Fermi level (the top panel of Fig. 6c), which represents the configuration wherein the extra non-bonding electron lies near the $N^+$. Another is the weak impurity state up the Fermi level (the top panel of Fig. 6c), which denotes the configuration in which the extra non-bonding electron lies at the edge atom and occupy the lowest unpaired $\pi^*$ edge electron level (the middle panel of Fig. 6c).

It is noted that there are sharp dips around the impurity states (especially for N5, N6 and N7 configuration) in Fig. 5. For the graphene, the local impurity state characterized by the resonance state, which is caused by the impurity perturbation, can even opens a quasi-gap in the vicinity of the nodal point [43,44]. And a weak scatter can cause a quasi-localized state and consequently a zero-conductance dip near the Fermi level in a ZCNR with non-magnetic impurity [38,45]. Hence, for 7-ZCNR with one substitutional nitrogen atom, the density of states in Fig. 5 produces the sharp dip near the impurity state and shows crucial dependence on the position of the impurity.

## 4. Conclusions

The formation energies and electronic properties for ZCNRs with one substitutional nitrogen atom per 154 carbon atoms depend on the nitrogen doping site, and the nitrogen atom energetically prefers to lie on the nanoribbon edge. The substitutional nitrogen atom near nanoribbon edges leads to that an impurity state appears below the Fermi level, while in others cases an impurity state locates above the Fermi level. The energy level of impurity states depend on both the coulomb attraction of $N^+$ and the correlation of unpaired $\pi$ edge electrons with the extra non-bonding electron in N atom, and the distance between the nitrogen atom and the ribbon edge decides to the sign change of the impurity energy level. These results suggest that one way to control the electronic property of ZCNRs by adjusting nitrogen doping sites can be realized.

## Acknowledgements

Supports from National Natural Science Foundation of China (Grant No. 50525204 and 50372024), the National Key Basic Research and Development Program (Grant Nos. 2004CB619301), Project 985 – Automotive Engineering of Jilin University, and the Teaching and Research Award Program for the Outstanding Young Teachers in High Education Institutions (Grant No. 2002359), are acknowledged.

## REFERENCES

[1] Wakabayashi K, Fujita M, Ajiki H, Sigrist M. Electronic and magnetic properties of nanographite ribbons. Phys Rev B 1999;59(12):8271–82.
[2] Barone V, Hod O, Scusera GE. Electron structure and stability of semiconducting graphene nanoribbons. NanoLetter 2006;6(12):2748–54.
[3] Nakada K, Fujita M, Dresselhaus G, Dresselhaus MS. Edge state in graphene ribbons: nanometer size effect and edge shape dependence. Phys Rev B 1996;54(24):17954–60.
[4] Lee YL, Lee YW. Ground state of graphite ribbons with zigzag edges. Phys Rev B 2002;66(24):245402-1–6.
[5] Miyamoto Y, Nakada K, Fujita M. First-principles study of edge states of H-terminated graphitic ribbons. Phys Rev B 1999;59(15):9858–61.
[6] Son YW, Cohen ML, Louie SG. Energy gaps in graphene nanoribbons. Phys Rev Lett 2006;97(21):216803-1–4.
[7] White CT, Li J, Gunlycke D, Mintmire JW. Hidden one-electron interactions in carbon nanotubes revealed in graphene nanostrips. NanoLetter 2007;7(03):825–30.
[8] Brey L, Fertig HA. Electronic states of graphene nanoribbons studied with the Dirac equation. Phys Rev B 2006;73(23):235411-1–5.
[9] Ezawa M. Peculiar width dependence of the electronic properties of carbon nanoribbons. Phys Rev B 2006;73(4):045432-1–8.
[10] Ramprasad R, Allmen PV, Fonseca LRC. A density-functional study of adsorbates at graphene ribbon edges. Phys Rev B 1999;60(8):6023–7.
[11] Kawai T, Miyamoto Y, Sugino O, Koga Y. Graphitic ribbon without hydrogen-termination: electronic structures and stabilities. Phys Rev B 2000;62(24):R16349–52.
[12] Martins TB, Miwa RH, da Silva AJR, Fazzio A. Electronic and transport properties of boron-doped graphene nanoribbons. Phys Rev Lett 2007;98(19):196803-1–4.
[13] Lee H, Son YW, Park N, Han S, Yu J. Magnetic ordering at the edges of graphitic fragments: magnetic tail interactions between the edge-localized states. Phys Rev B 2005;72(17):174431-1–8.
[14] Novoselov KS, Geim AK, Morozov SV, Jiang D, Katsnelson MI, Grigoerva V, et al. Two-dimensional gas of massless Dirac fermions in graphene. Nature 2005;438(7065):197–200.
[15] Zhang YB, Tan YW, Stormer HL, Kim P. Experimental observation of the quantum Hall effect and Berry's phase in graphene. Nature 2005;438(7065):201–4.
[16] Stankovich S, Dikin DA, Dommett GHB, Kohlhaas KM, Zimney EJ, Stach EA, et al. Graphene-based composite materials. Nature 2006;442(7100):282–6.
[17] Niimi Y, Matsui T, Kambara H, Tagami K, Tsukada M, Fukuyama H. Scanning tunneling microscopy and spectroscopy of the electronic local density of states of graphite surfaces near monoatomic step edges. Phys Rev B 2006;73(8):085421-1–8.
[18] Kobayashi Y, Fukui KI, Enoki T, Kusakabe K. Edge state on hydrogen-terminated graphite edges investigated by scanning tunneling microscopy. Phys Rev B 2006;73(12):125415-1–8.
[19] Wilson M. Electrons in atomically thin carbon sheets behave like massless particles. Phys Today 2006;59(1):21–3.

[20] Wang ZF, Li QX, Zheng HX, Ren H, Su HB, Shi QW, et al. Tuning the electronic structure of graphene nanoribbons through chemical edge modification: a theoretical study. Phys Rev B 2007;75(11):113406-1–4.
[21] Ma YC, Foster AS, Krasheninnikov AV, Nieminen RM. Nitrogen in graphite and carbon nanotubes: magnetism and mobility. Phys Rev B 2005;72(20):205416-1–6.
[22] Shimoyama I, Wu GH, Sekiguchi T, Baba Y. Evidence for the existence of nitrogen-substituted graphite structure by polarization dependence of near-edge X-ray-absorption fine structure. Phys Rev B 2000;62(10):R6053–6.
[23] Snis A, Mater SF. Electronic density of states, 1s core-level shifts, and core ionization energies of graphite, diamond, $C_3N_4$ phases, and graphitic $C_{11}N_4$. Phys Rev B 1999;60(15):10855–63.
[24] Hellgren N, Johansson MP, Broitman E, Hultman L, Sundgren JE. Role of nitrogen in the formation of hard and elastic $CN_x$ thin films by reactive magnetron sputtering. Phys Rev B 1999;59(7):5162–9.
[25] Santo MC dos, Alvarez F. Nitrogen substitution of carbon in graphite: structure evolution toward molecular forms. Phys Rev B 1998;58(20):13918–24.
[26] Mazzoni MSC, Nunes RW, Azevedo S, Chacham H. Electronic structure and energetics of $B_xC_yN_z$ layered structures. Phys Rev B 2006;73(7):073108-1–4.
[27] Stafstrom Sven. Reactivity of curved and planar carbon-nitride structures. Appl Phys Lett 2000;77(24):3941–3.
[28] Dresselhaus MS, Dresselhaus G, Avouris P. Carbon nanotubes, synthesis, structure, properties and applications. Berlin: Springer; 2001.
[29] Nevidomskyy AH, Csányi C, Payne MC. Chemically active substitutional nitrogen impurity in carbon nanotubes. Phys Rev Lett 2003;91(10):105502-1–4.
[30] Droppa Jr R, Ribeiro CTM, Zanatta AR, Santos MC dos, Alvarez F. Comprehensive spectroscopic study of nitrogenated carbon nanotubes. Phys Rev B 2004;69(4):045405-1–9.
[31] Jang JW, Lee CE, Lyu SC, Lee TJ, Lee CJ. Structural study of nitrogen-doping effects in bamboo-shaped multiwalled carbon nanotubes. Appl Phys Lett 2004;84(15):2877–9.
[32] Terrones M, Ajayan PM, Banhart F, Blase X, Carroll DL, Charlier JC, et al. N-doping and coalescence of carbon nanotubes: synthesis and electronic properties. Appl Phys A 2002;74(3):355–61.
[33] Kaun CC, Larade B, Mehrez H, Taylor J, Guo H. Current–voltage characteristics of carbon nanotubes with substitutional nitrogen. Phys Rev B 2002;65(20):205416-1–5.
[34] Zhao M, Xia YY, Lewis JP, Zhang R. First-principles calculations for nitrogen-containing single-walled carbon nanotubes. J Appl Phys 2003;94(4):2398–402.
[35] Han W, Bando Y, Kurashima K. Boron-doped carbon nanotubes prepared through a substitution reaction. Chem Phys Lett 1999;299(5):368–73.
[36] Yu SS, Wen QB, Zheng WT, Jiang Q. Effects of doping nitrogen atoms on the structure and electronic properties of zigzag single-walled carbon nanotubes through first-principles calculations. Nanotechnology 2007;18(16):165702-1–7.
[37] Yi JY, Bernholc J. Atomic structure and doping of microtubules. Phys Rev B 1993;47(3):1708–11.
[38] Wakabayshi K. Numerical study of the lattice vacancy effects on the single-channel electron transport of graphite ribbons. J Phys Soc Jpn 2002;71(10):2500–4.
[39] Delley B. An all-electron numerical method for solving the local density functional for polyatomic molecules. J Chem Phys 1990;92(1):508–17.
[40] Delley B. From molecules to solids with the Dmol3 approach. J Chem Phys 2000;113(18):7756–64.
[41] Perdew JP, Burke K, Ernzerhof M. Generalized gradient approximation made simple. Phys Rev Lett 1996;77(18):3865–8.
[42] Jiang DE, Sumpter BG, Dai S. Unique chemical reactivity of a graphene nanoribbon's zigzag edge. J Chem Phys 2007;126(13):134701-1–6.
[43] Skrypnyk YV, Loktev VM. Impurity effects in a two-dimensional system with the Dirac spectrum. Phys Rev B 2006;73(24):241402-1–4.
[44] Wehling TO, Balatsky AV, Katsnelson MI, Lichtenstein AI, Scharnberg K, Wiesendanger R. Local electronic signatures of impurity states in graphene. Phys Rev B 2007;75(12):125425-1–5.
[45] Li TC, Lu SP. Quantum conductance of graphene nanoribbons with edge defects. Available from: <cond-mat/0609009 v1>.